Bachelor Thesis:

The p-T-phase diagram of the NJL model at real and imaginary chemical potential

Kilian Keilholz

21.02.2013

Technische Universität Darmstadt

Fachbereich Physik
Institut für Kernphysik - Theoriezentrum
Schlossgartenstraße 2
64289 Darmstadt

1. Gutachten: PD Dr. Michael Buballa
2. Gutachten: Prof. Dr. Jochen Wambach

Tag der Einreichung: 21.02.2013

Abstract

In the following work, the NJL model for quark matter at finite temperature T and chemical potential μ is investigated and phase transitions are analyzed. Following approaches on the lattice, strictly imaginary chemical potentials $\mu \to i\mu$, shall be rendered in this model as well.
p-T-phase diagrams, showing the chiral phase transitions for real and imaginary chemical potential, are eventually acquired. Those diagrams are discussed and compared both, for finite quark mass $m \neq 0$ and in the chiral limit $m = 0$.
To reproduce the periodicities predicted by QCD and lattice calculations, the NJL model is further extended by the introduction of the Polyakov loop in the final part of this thesis.

Contents

Chapter 1

Introduction

As quarks shall be investigated in this work, the theory of quantum chromodynamics (QCD) gives the proper framework, describing the so called strong interaction between objects carrying color charge. Gluons act as transmission particles of this interaction and the fact that they themselves are carrying color gives rise to effects not found in electrodynamics, but also makes QCD a much more complex theory. In analogy to the electromagnetic interaction, where charged objects are striving after the energetically most favorable distribution of neutral electric charge, particles underlying the strong interaction are favoring arrangements of color neutrality. The color charge of the gluon itself gives rise to the effect of confinement, preventing the existence of constituent colored particles up to extreme thermodynamic environments which can only be recreated in modern particle colliders. Therefore the theory of QCD is still quite unaccessible to experiments and many insights and results can only be obtained by theoretical approaches such as lattice QCD.

By treating QCD in terms of thermodynamics a rather extensive phase diagram is found. At moderate pressure and temperature strictly coupled quarks (hadrons) exist, in more extreme environments those states evolve into a phase of free, deconfined quarks and glouns (quark-gluon plasma, QGP). Besides those there are more phases found or expected, including a crystalline as well as a color-superconducting phase.
A sketched overview can be found in [4]. Here the diagram is drawn in terms of pressure p over temperature T, as it is commonly done in classical thermodynamics. However, in QCD phase transitions are usually discussed in domains of temperature and chemical potential μ, a quantity that is not as graspable as the pressure. Therefore creating QCD phase diagrams for p over T allows a more direct comparison of the quite abstract quark matter to ordinary substances like water or gases.
As they are based on terms like gas, liquid, plasma or crystal, the denominations of the QCD phases already imply some analogies to the phases of classical matter.

To build the basis for treating properties of quarks and their interaction in a theoretical frame, the upcoming parts give an introduction to the required physics and establish the later applied NJL model.

1.1 Related QCD in brief

A general quark field in QCD with 6 flavor and 3 color degrees of freedom is described by its Lagrangian [5]:

$$\mathcal{L} = \overline{q}(i\gamma^\mu D_\mu - \widehat{m})q - \frac{1}{4}G^{a\mu\nu}G^a_{\mu\nu} \tag{1.1}$$

Here q describes the quark field with degrees of freedom in flavor and color space. $\hat{m} = diag(m_u, m_d, m_s, m_c, m_t, m_b)$ is the matrix of the bare quark masses.

Both, the covariant derivative

$$D_\mu = \partial_\mu - ig\frac{\lambda^a}{2}A^a_\mu \tag{1.2}$$

and the gluon field strength tensor

$$G^a_{\mu\nu} = \partial_\mu A^a_\nu - \partial_\nu A^a_\mu + gf^{abc}A^b_\mu A^c_\nu \tag{1.3}$$

are related to the gluon field A^a_μ.

g is the QCD coupling constant, f^{abc} are antisymmetric structure constants and λ^a denote the 8 Gell-Mann matrices, i.e. the generators of the SU(3) group.

This Lagrangian is symmetric under SU(3) gauge transformations in color space and unlike the QED Lagrangian it is not-Abelian.
The latter is manifested in effects like the self-coupling of gluons due to them carrying color and in the asymptotically free behavior of QCD, which means that the coupling becomes strong at high distances and weak at short distances (i.e. on subnuclear scales), allowing quarks to behave as nearly free particles. This actually is not necessarily related to the effect of confinement that prohibits the observation of constituent quarks.

Another important property of the QCD Lagrangian, especially regarding the later introduced NJL model, is the (approximate) chiral symmetry under global vector and axial-vector transformations[1] $\mathrm{SU(N}_f)_V \times \mathrm{SU(N}_f)_A$:

$$\begin{aligned} SU(N_f)_V &: q \to e^{(i\Theta^V_a \tau_a)}\, q \\ SU(N_f)_A &: q \to e^{(i\Theta^A_a \gamma_5 \tau_a)}\, q \end{aligned} \tag{1.4}$$

[1] These derive from left and right hand transformations $\mathrm{SU(N}_f)_L \times \mathrm{SU(N}_f)_R$: $\psi_L(x) \to e^{-i\Theta^L_a \tau^a}\psi_L(x)$, $\psi_R(x) \to e^{-i\Theta^R_a \tau^a}\psi_R(x)$, see [10].

with τ_a the generators of the flavor space $\mathrm{SU(N}_f)$ and $\gamma_5 = i\gamma_0\gamma_1\gamma_2\gamma_3$, where γ_j are the 4×4-matrices introduced in the Dirac formalism.
This symmetry would be exact only for massless quarks, which is not the case for any quark type. But as the proposed masses for constituent u- and d-quarks are rather small[1] ($m_u \sim 2.5\,\mathrm{MeV}$ and $m_d \sim 5.0\,\mathrm{MeV}$), it is still approximately satisfied and can be investigated by restricting the model to those light particles. To fully realize this symmetry by the model, one can consider the chiral limit $m = 0$.

Because of the non-existence of non-degenerate chiral partners with opposite parity for hadrons[1], one postulates a spontaneous breaking of chiral symmetry in vaccuum, which is restored in thermodynamic environments of high T and μ. The chiral condensate $\langle\overline{q}q\rangle$, which is not invariant under $\mathrm{SU(N}_f)_A$ transformations, represents an order parameter for this symmetry breaking.

1.2 The NJL model

The NJL model was established by Y. Nambu and G. Jona-Lasinio in 1960/61, at first to describe the mass of Dirac particles (e.g. nucleons) as a result of the self-energy of a postulated primary fermion field [6].
It was later interpreted as a model for quarks[2] and their interactions, reflecting the properties connected to chirality (i.e. chiral symmetry for massless fermions and spontaneous breaking of chiral symmetry for fermions with mass).
In this quark model, gluons as mediators of the strong force are ignored, therefore the property of confinement is not reproduced.

By restricting the NJL model on the light u- and d-quark, the associated Lagrangian is of the form:

$$\mathcal{L}_{NJL} = \overline{q}(i\gamma^\mu\partial_\mu - \widehat{m})q + G[(\overline{q}q)^2 + (\overline{q}i\gamma_5\vec{\tau}q)^2] \tag{1.5}$$

where the mass-matrix $\widehat{m} = diag(m_u, m_d)$ can be simplified to $\widehat{m} = \mathrm{Id}(m)$ by assuming the same mass m for both flavors.
Comparing this to the generic QCD Lagrangian (1.1) illustrates the omission of the gluon field A^a_μ in both, the free and the interaction part.
The latter is here assumed as a point-like four-fermion interaction whose self-energy gives rise to an effective mass M that can take on much higher values than the bare mass m.
This effective mass depends on the trace over the quark propagator $S(p)$:

$$M = m + 2iG\int \frac{d^4p}{(2\pi)^4}\, tr\, S(p) \tag{1.6}$$

[1] The given values are in accordance to http://pdg.web.cern.ch/pdg/2011/reviews/rpp2011-rev-quark-masses.pdf

[2] Quarks had not been postulated as elementary particles until around 1965.

where in Hartree or Hartree-Fock approximation this dressed propagator $S(p) = \dfrac{1}{\not{p} - M + i\epsilon}$ is described by the Dyson equation fig. 1.1

Figure 1.1: Dyson equation of the dressed quark propagator $S(p)$ (bold) which is constituted of the bare propagator with mass m (thin) and a self-energy loop (second term on the right hand side); excerpt of [1]

As the trace in (1.6) needs to be taken in Dirac, flavor and color space, this yields an additional factor of $4N_f N_c$ which gives a self-consistent function for the effective mass:

$$M = m + 8N_f N_c iG \int \frac{d^4p}{(2\pi)^4} \frac{M}{p^2 - M^2 + i\epsilon} \tag{1.7}$$

1.2.1 The grand canonical potential Ω_{NJL}

In order to find the effective mass M for different thermodynamic environments, the grand canonical potential Ω_{NJL} shall be introduced to investigate the NJL model in terms of temperature T and chemical potential μ.

The general definition of the grand canonical potential is given as [1]:

$$\Omega(T, \mu) := -\frac{T}{V} \ln \left[tr\, exp\left(-\frac{1}{T} \int d^3x \left(\mathcal{H} - \mu q^\dagger q \right) \right) \right] \tag{1.8}$$

where $\mathcal{H}$ is the Hamiltonian density and the trace tr needs to be taken over all states of the system. Introducing the quark condensate $\sigma := \langle \overline{q}q \rangle$ and assuming $\overline{q}q = \langle \overline{q}q \rangle + \delta\overline{q}q$:

$$(\overline{q}q)^2 \approx \langle \overline{q}q \rangle^2 + 2\langle \overline{q}q \rangle \delta\overline{q}q = 2\sigma\overline{q}q - \sigma^2 \tag{1.9}$$

eq. (1.5) gives:

$$\mathcal{L} = \overline{q} \left(i\gamma^\nu \partial_\nu - (m - 2G\sigma) \right) q - G\sigma^2 \tag{1.10}$$

Here the term $(\overline{q} i\gamma_5 \vec{\tau} q)^2$ is assumed to vanish.

Now defining the effective mass $M := m - 2G\sigma$ and introducing the chemical potential μ in terms of an extension $\mu q^\dagger q$ eq. (1.10) takes the following form:

$$\mathcal{L} + \mu q^\dagger q = \overline{q}(i\gamma^\nu \partial_\nu - M)q + \mu q^\dagger q - \frac{(M - m)^2}{4G} \tag{1.11}$$

This is now equivalent to the description of a system of non-interacting particles with mass M and a potential term $\frac{(M-m)^2}{4G}$ independent of q [1], the according thermodynamic potential is given as:

$$\Omega(T,\mu;M) = \Omega_M(T,\mu) + \frac{(M-m)^2}{4G} \tag{1.12}$$

where Ω_M denotes the free Fermi-gas contribution:

$$\Omega_M(T,\mu) = -T\sum_n \int \frac{d^3p}{(2\pi)^3}\, tr\left(\frac{1}{T}\,\ln\left[S^{-1}(i\omega_n,\vec{p})\right]\right) \tag{1.13}$$

$S^{-1} = \gamma^\nu\partial_\nu - \mu\gamma^0 - M$ is the inverse fermion propagator at chemical potential μ. It has to be evaluated for the 0-component p^0 of the four-momentum p taking on the fermionic Matsubara frequencies $i\omega_n = (2n+1)\pi T$.

Introducing $E(p) := \sqrt{\vec{p}^2 + M^2}$ and following [1] and [3] gives[1]:

$$\Omega_M(T,\mu) = \\ -2N_fN_c\int \frac{dp^3}{(2\pi)^3}\left\{E(p) + T\left[ln\left(1+e^{-\frac{E(p)+\mu}{T}}\right) + ln\left(1+e^{-\frac{E(p)-\mu}{T}}\right)\right]\right\} \tag{1.14}$$

So the grand canonical potential of the NJL Lagrangian eq. (1.5) is eventually found to be:

$$\widetilde{\Omega}_{NJL}(T,\mu;M) = \\ \frac{(M-m)^2}{4G} - 2N_fN_c\cdot \\ \cdot\int \frac{dp^3}{(2\pi)^3}\left\{E(p) + T\left[ln\left(1+e^{-\frac{E(p)+\mu}{T}}\right) + ln\left(1+e^{-\frac{E(p)-\mu}{T}}\right)\right]\right\} \tag{1.15}$$

Where $N_c = 3$, $N_f = 2$ denote the number of colors and flavors and $E(p) = \sqrt{p^2+M^2}$.

As the first term under the integral yields $\sim \int p^2\sqrt{p^2+M^2}\,dp$, which is diverging, the integral has to be regularized. In the case at hand, this is done by the introduction of an arbitrary sharp three-momentum cut-off λ for the upper limit of integration:

$$\int_{\mathbb{R}^3}\frac{dp^3}{(2\pi)^3} \longrightarrow \int_{|p|\leq\lambda}\frac{dp^3}{(2\pi)^3} \;=\; \int_0^\lambda \frac{4\pi|p|^2}{(2\pi)^3}\,d|p| \tag{1.16}$$

[1] The detailed steps are rather complex and extensive, a further discussion can be found in the given references.

Applying this cut-off only for the first term under the integral yields the regularized grand canonical potential[1]:

$$\Omega_{NJL}(T,\mu;M) = \frac{(M-m)^2}{4G} - 2N_f N_c \frac{4\pi}{(2\pi)^3}\cdot \cdot\{\int_0^\lambda dp\, p^2 E(p) \; + \int_0^\infty dp\, p^2\, T\left[ln\left(1+e^{-\frac{E(p)+\mu}{T}}\right) + ln\left(1+e^{-\frac{E(p)-\mu}{T}}\right)\right]\} \tag{1.17}$$

The coupling factor G, the bare quark mass m and the cut-off λ are free parameters which have to be fixed for further practical evaluations. Convenient choices are acquired by fitting the NJL model to results of lattice calculations or by reproducing specific properties of known quantities.
The latter is done here by adopting a set (λ, m, G) that reproduces the mass, the decay constant of the pion and the quark condensate [1]:

λ	587.9 MeV
m	5.6 MeV
G	$2.44/\lambda^2$

For physical solutions the grand canonical potential $\Omega_{NJL}(T,\mu;M)$ always takes its (global) minimal value, so for fixed T and μ the physical constituent quark mass M can be obtained by solving

$$\frac{\partial\Omega_{NJL}(T,\mu;M)}{\partial M} = 0 \tag{1.18}$$

$$\Longleftrightarrow$$

$$\frac{M-m}{2G} - 2N_f N_c \frac{4\pi}{(2\pi)^3}\cdot \cdot\{\int_0^\lambda dp\, p^2 \frac{M}{E(p)} - \int_0^\infty dp\, p^2 \frac{M}{E(p)}\left(\frac{1}{1+e^{\frac{E(p)+\mu}{T}}} + \frac{1}{1+e^{\frac{E(p)-\mu}{T}}}\right)\} = 0 \tag{1.19}$$

For zero temperature and chemical potential, this so called gap equation[2] is in fact equivalent to eq. (1.7) derived by the Dyson equation fig. 1.1.
As it is self-consistent for M it can in general have more than one solution.
Evaluating Ω_{NJL} at those points eventually yields the global minimum and therefore the physical value of M.

[1] for convenience, p in the following passages denotes the absolute value $|\vec{p}|$ of the three-momentum

[2] inspired by the analogy of the behavior of the constituent quark mass to the energy gap of Cooper pairs in BCS-theory

Chapter 2

Numerical Calculations

2.1 Calculations at real chemical potential

The behaviour of the grand canonical potential Ω_{NJL} is examined by numerically evaluating the gap equation (1.18) for real chemical potential μ.

2.1.1 for non-vanishing $m = 5.6\,\mathrm{MeV}$

Setting the bare quark mass $m = 5.6\,\mathrm{MeV}$, the constituent masses M, minimizing $\Omega_{NJL}(T, \mu; M)$, are plotted over the T-μ-plane:

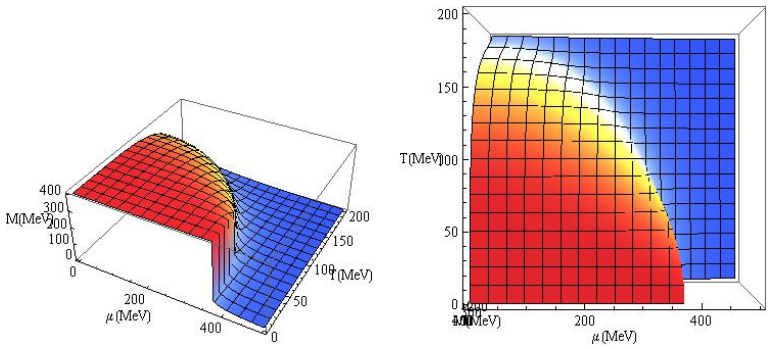

Figure 2.1: Effective mass M over T-μ-plane for non-vanishing bare quark mass $m = 5.6\,\mathrm{MeV}$

Narrowing down the areas of the T-μ-plane where M is changing sharply in direction along the μ-axis yields a 1st order transition at low temperature T and high values of μ, evolving in a crossover transition at increasing T, decreasing μ. The crossover is defined by the maximal slope of the curve along the μ-axis.

In domains of T and μ this yields the following phase diagram:

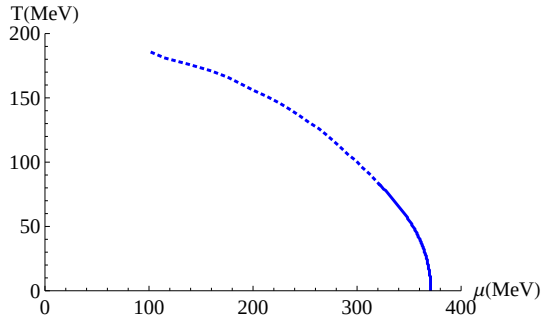

Figure 2.2: (T, μ) phase diagram for bare quark mass $m = 5.6\,\text{MeV}$. The solid line represents the 1st order transition, the dotted one the crossover transition

The critical end point (CEP) of the first order transition is found at $(T,\ \mu) = (82.6\,\text{MeV},\ 321.5\,\text{MeV})$. As the crossover transition along the μ-axis becomes less and less incisive at low chemical potentials, it is by convention restricted to points (T,μ) where the slope takes reasonably high values[1], therefore it does not reach out to values of $\mu \sim 0$.[2]

2.1.2 in the chiral limit, $m = 0$

Considering the bare quark mass in the chiral limit $m = 0$ yields at first a quite similar picture as in the case of non-zero m:

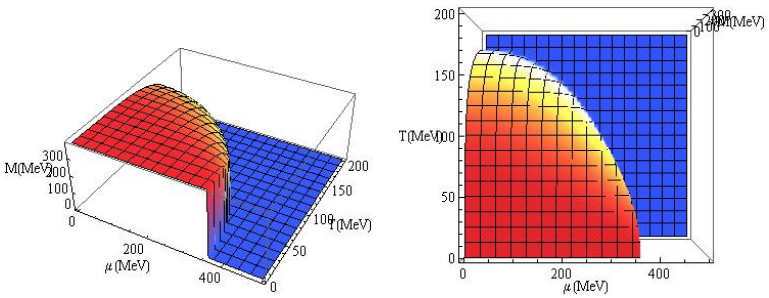

Figure 2.3: Effective mass M over T-μ-plane in the chiral limit $m = 0$

Comparing this against fig. (2.1) however, the effective mass drops much sharper. This is seen clearly especially in the high T, low μ region on the top-view of the right hand side picture of fig. (2.3).

[1] The criterion for this is chosen to be $\frac{dM}{d\mu} \sim 100$.

[2] As will be seen in 2.3, it might be interesting to define down the criterion for the crossover transition to extend this diagram.

A more proper analysis by narrowing down the T-μ-plane around the points of high slope along the μ-axis now indicates phase transitions of 1st and 2nd order and, other than in the preceding case, the 2nd order transition can be easily determined up to zero chemical potential μ as no crossover convention has to be introduced.
In domains of (T, μ) the following phase diagram is obtained:

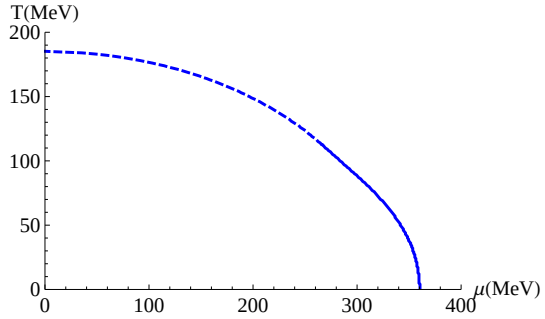

Figure 2.4: (T, μ) phase diagram in chiral limit $m = 0$. The solid line represents the 1st order transition, the dashed one the 2nd order transition

This yields not only a tricritical end point of the 1st order transition at $(T,\ \mu) = (112.6\,\text{MeV},\ 266.4\,\text{MeV})$, but also an absolute critical temperature $T_0 = 185.2\,\text{MeV}$, above which the chiral symmetry is restored for any value of μ.

2.2 Calculations at imaginary chemical potential $\mu \to i\mu$

Due to the sign problem for Monte Carlo simulations[1], approaches on the lattice are not feasible for chemical potentials $\mu^2 > 0$ $(*)$. Therefore an imaginary chemical potential $\mu \to i\mu$ is introduced.
At first this seems unphysical, but allows calculations at $\mu \neq 0$ circumventing the limitation $(*)$, those can then be extrapolated to real values of μ.

By implementing the imaginary chemical potential $i\mu$ in the NJL potential eq. (1.17) it is convenient to introduce $\Theta := \frac{\mu}{T}$ as variable, reflecting the phase of

[1] For $\mu \neq 0$ the determinant $\det(\not{D} + m + \mu\gamma_0)$ showing up in the partition function takes on complex values. This however inhibits the Monte Carlo methods for lattice QCD simulations. More details on this topic are given in [11], [12]

the emerging imaginary exponents:

$$\Omega_{NJL}(T,\Theta;M) = \frac{(M-m)^2}{4G} - 2N_f N_c \frac{4\pi}{(2\pi)^3}\cdot$$
$$\cdot\{\int_0^\lambda dp\, p^2\sqrt{p^2+M^2} + \int_0^\infty dp\, p^2 T\left[\ln(1+e^{-\frac{E(p)}{T}}e^{-i\Theta}) + \ln(1+e^{-\frac{E(p)}{T}}e^{i\Theta})\right]\} \tag{2.1}$$

$\Omega_{NJL}(T,\Theta;M)$ is a real function[1] as each complex exponential function appears with its complex conjugate (compare appendix [A]).
Applying the parameter set (λ, m, G) as introduced in 1.2.1 allows calculations by now fixing T and Θ and searching for minimal values of Ω_{NJL} in analogy to the case of real μ.

2.2.1 for non-vanishing $m = 5.6\,\mathrm{MeV}$

Choosing the non-zero bare quark mass $m = 5.6\,\mathrm{MeV}$, transitions are found in domains of T and Θ according to figure (2.5). Those are merely crossover transitions, with the maximum curvature along the Θ-axis[2] set as criterion.
The points show an exact mirrored behavior following $M(T,\Theta) = M(T, 2\pi - \Theta)$, which is due to the terms $\sim e^{\pm i\Theta}$ in Ω_{NJL}[3].

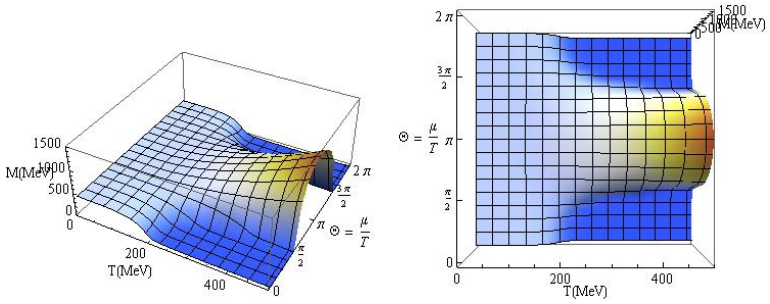

Figure 2.5: Effective mass M over T-Θ-plane for bare quark mass $m = 5.6\,\mathrm{MeV}$ in the case of imaginary chemical potential

A more detailed evaluation shows that only a crossover transition occurs, the according transition lines in (T,Θ)-domain are shown in fig. (2.6).

[1] The grand canonical potential Ω always has to take real values as it represents the physical value of pressure (up to a constant).

[2] For the points around $T = 200\,\mathrm{MeV}$ the curvature along the T-axis is investigated. However, as can be seen in the upcoming diagrams, those transition points match well with the behavior of the transition points obtained for the curvature along the Θ-axis.

[3] As Ω_{NJL} is a real function, this is already intuitively clear:
$Re[e^{\pm i\Theta}] = \cos(\pm\Theta)$ and $\cos(\theta) = \cos(2\pi - \theta)$, reflecting the mentioned symmetry. A more detailed explanation is given in appendix [A].

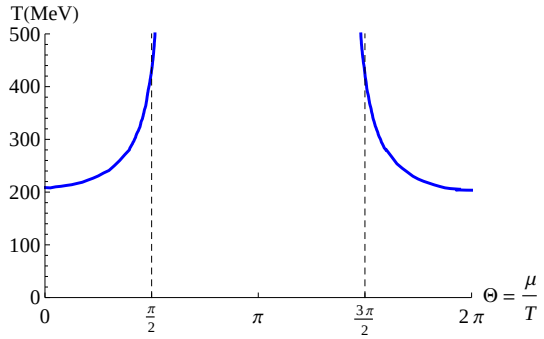

Figure 2.6: (T, μ) phase diagram for bare quark mass $m = 5.6\,\mathrm{MeV}$ in the case of imaginary chemical potential μ. The transition is strictly a crossover type.

Here a critical temperature $T_0 \simeq 205\,\mathrm{MeV}$ is found, below which it is not possible at any value of Θ to find the (approximate) restoration of chiral symmetry $M \to 0$.

2.2.2 in the chiral limit, $m = 0$

As in the cases of real chemical potential, the behavior of the effective mass M in the chiral limit is similar compared to the results at non-vanishing bare mass:

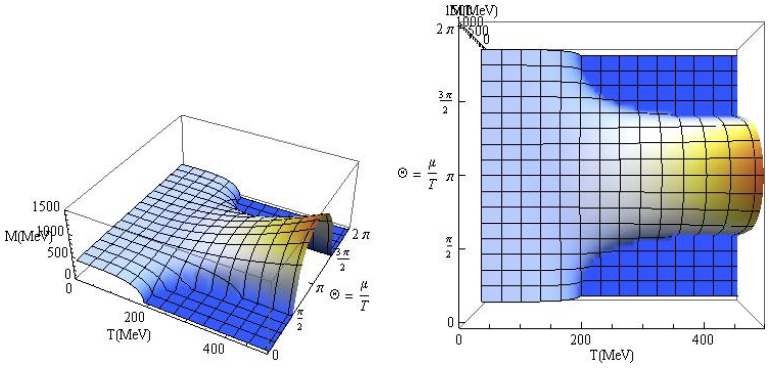

Figure 2.7: Effective mass M over T-Θ-plane for the chiral limit $m = 0$ in the case of imaginary chemical potential

The crossover transition in fig. (2.5),(2.6) changes into a transition strictly of 2nd order. This can be seen in fig. (2.7) on the left hand picture where for small Θ the transition along the T-axis has a cusp that is not found in the case of non-vanishing bare mass m.

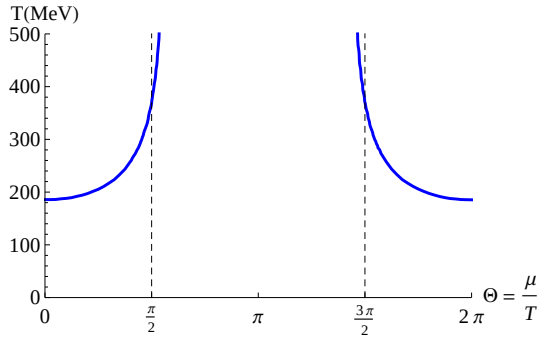

Figure 2.8: (T, μ) phase diagram for chiral limit $m = 0$ in the case of imaginary chemical potential μ. The transition is strictly a 2nd order type.

The critical temperature is found at a slightly lower value than in the case of $m = 5.6\,\mathrm{MeV}$: $T_0 \simeq 185.6\,\mathrm{MeV}$.

2.3 Phase diagrams in domains of p and T

The pressure p is connected to the physical value of the grand canonical potential Ω_{NJL} by

$$p(T, \mu) = -\,\Omega_{NJL}(T, \mu; M_{min}(T, \mu)) - p_0 \tag{2.2}$$

where M_{min} denotes the physical value of the constituent quark mass minimizing Ω_{NJL} in a thermodynamic environment of (T, μ). p_0 is the zero pressure, which is conveniently defined as $p_0 := \Omega_{NJL}(T = 0, \mu = 0; M_{min})$, such that $p(0, 0) = 0$.

Applying eq. (2.2) to the points (T,μ) determining the phase transitions yields the diagram in the p-T-plane[1].

For a fixed temperature a system at zero chemical potential μ always takes the lowest possible pressure. Therefore by setting $\mu = 0$ and evaluating[2] Ω_{NJL} for T, a limiting line is found for the minimal pressure that should be expected for physical solutions.
In this context, values below this line have to be considered unphysical. The upcoming results for imaginary μ, which are strictly speaking unphysical, are in fact found in this realm.

[1] Of course this also holds in analogy for the points (T, Θ) in the imaginary case.

[2] Evaluating in this case means finding the physical constituent mass M minimizing the grand canonical potential for each fixed T and computing Ω_{NJL} for this point $(T, 0, M)$, which is done in analogy to the preceeding calculations at non-vanishing μ.

Assembling the obtained phase phase transitions for both cases of real and imaginary chemical potential yields the following p-T-diagrams:

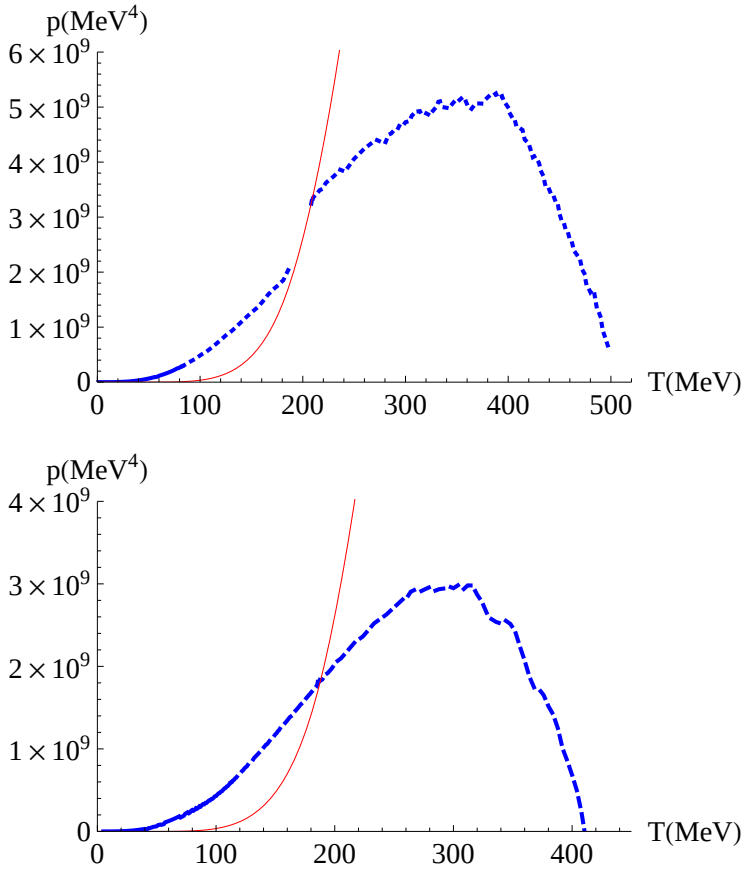

Figure 2.9: Phase diagrams in domains of (p, T) acquired by combining the evaluated transitions for both, real and imaginary μ.
Top: for non-vanishing bare mass $m = 5.6\,\mathrm{MeV}$, where the 1st order transition (solid line) evolves into a crossover type (dotted) at the CEP at $T_0 = 82.6\,\mathrm{MeV}$.
Bottom: in the chiral limit $m = 0$, here the 1st order transition evolves into a 2nd order type (dashed) at $T_0 = 112.6\,\mathrm{MeV}$, note the smooth passage from the physical ($\mu^2 > 0$) to the unphysical ($\mu^2 < 0$) domain.

As the evaluated diagrams fig. (2.9) show, the transitions for strictly imaginary chemical potential are all restricted to the unphysical area. For means of comparison the limiting line discussed before is indicated in red in both diagrams. The unsteady behavior in the imaginary realm is most likely caused by the numerical methods of computation and the fact that the points of the phase transition are only accurate up to a finite extent as all calculations can only be

realized for discrete values of T and μ.
It is noticable that the transition from the physical to the unphysical domain is smooth in case of the chiral limit. However, it is clear that the curve has to be continuous at this point, as eq. (1.17) at $\mu = 0$ is equivalent to eq. (2.1) at $\Theta = \frac{\mu}{T} = 0$.
In case of non-vanishing bare mass the curve should also be continuous, but whether it has a cusp at this point can not be concluded as, because of the introduction of the crossover criterion, the corresponding transition for real μ could not be extended up to its limit (compare section 2.1 and fig.(2.2)).
To check whether the behavior is smooth or not, it might be interesting to investigate the crossover transition for the missing section in fig. (2.2) and (2.9) more precisely by defining a more generous crossover criterion or by evaluating the transition points for the maximum slope in direction of the T-axis.

Chapter 3

Outlook: The PNJL extension

As discussed before, in the NJL model gluons are neglected, therefore some effects, most notably the property of confinement, are not reproduced by assuming the Lagrangian eq. (1.5).
Also, at imaginary chemical potential, the SU(3) gauge theory has a periodicity of $\frac{2\pi}{3}$ [8], which obviously is not shown in the results of section 2.2, where a periodicity of 2π is found.
To implement confinement, the so called Polyakov loop shall be introduced as an extension to the NJL model. Thereby the correct periodicity also emerges eventually.

3.1 The Polyakov loop

In a confined system color charged asymptotic states are absent, which can be described by the free energy F_q of constituent quarks. Assuming infinitely heavy quarks, this means that in the confined phase an infinite amount of energy is needed to add a single quark to a system, whereas in the deconfined phase a finite energy is sufficient.
The operator describing the creation of a single quark is related to the trace over the Polyakov loop $\mathcal{P}\, e^{i\int_0^{\frac{1}{T}} d\tau\, A_4}$ [13]:

$$L = \frac{1}{N_c}\, tr\left[\mathcal{P}\, e^{i\int_0^{\frac{1}{T}} d\tau\, A_4}\right] \tag{3.1}$$

with $A_4 = iA_0 = i\delta_{\mu 0} g A_a^\mu \frac{\lambda^a}{2}$ a 3×3-matrix in color space, where A_a^μ represents the gauge field and $\mathcal{P}$ denotes the path ordering.

In the Polyakov gauge the actual loop $\mathcal{P}\, e^{i\int_0^{\frac{1}{T}} d\tau\, A_4}$ can be written in a diagonal

representation, such that for $N_c = 3$

$$L = \frac{1}{3}\, tr\left[e^{i\Lambda}\right] \tag{3.2}$$

where $\Lambda = B_3\lambda_3 + B_8\lambda_8$ with λ_3 and λ_8 the two diagonal Gell-Mann matrizes. Therefore the traced Polyakov loop is a function $\Phi(B_3, B_8)$ of the two field variables B_3 and B_8.
The expectation values $\Phi = \langle L\rangle$ and $\overline{\Phi} = \langle L^\dagger\rangle$ are related to the free energy F_q, $F_{\overline{q}}$ of a single quark and anti-quark respectively:

$$\Phi \sim e^{-\frac{F_q}{T}}, \quad \overline{\Phi} \sim e^{-\frac{F_{\overline{q}}}{T}} \tag{3.3}$$

This reflects the mentioned connection to the operator describing the creation of single quarks:
In a confined system the free energy is infinitely high, implying $\Phi \to 0$. In a deconfined environment, where single quarks can be created, the finite free energy gives an expection value $\Phi \neq 0$.

So in this context, the traced expectation values Φ and $\overline{\Phi}$ of the Polyakov loop represent an order parameter of the confinement-deconfinement phase transition.
As the relation between confinement and the free energy of a single quark was proposed for the assumption of infinitely heavy quarks, it is actually only an approximate order parameter for this phase transition. Following [8] and [13] it shall be applied nonetheless.
It is notable that no formalism for gluons had to be introduced to describe the property of confinement.

3.2 The PNJL Lagrangian and grand canonical potential

As the NJL model of section 1.2 describes the chiral phase transition and the Polyakov loop gives a model for the property of confinement, an extension of the simple NJL Lagrangian eq. (1.5) by implementing the traced Polyakov loop expectation values Φ, $\overline{\Phi}$ gives a more complete picture.
It reproduces the properties of chiral symmetry (i.e. its breaking and restoration) as well as confinement.

Extending the NJL Lagrangian with the Polyakov potential $\mathcal{U}(\Phi, \overline{\Phi}, T)$ following [8] yields:

$$\mathcal{L}_{PNJL} = \overline{q}(i\gamma_\nu D^\nu - m)q + G\left[(\overline{q}q)^2 + (\overline{q}i\gamma_5\vec{\tau}q)^2\right] - \mathcal{U}(\Phi, \overline{\Phi}, T) \tag{3.4}$$

where $D^\nu = \partial^\nu - iA^\nu$ with the field $A^\nu = \delta_{\nu 0} g A^\nu_a \frac{\lambda^a}{2}$.
This has the same structure as eq. (1.5), only the derivative in the free Dirac

term is extended with the gauge field A^ν and a potential term $\mathcal{U}(\Phi, \overline{\Phi}, T)$ independent of q, $\overline{q}$ is added due to the Polyakov loop Φ.

Assuming mean field approximation and introducing the chiral condensate $\sigma := \langle \overline{q} q \rangle$ as well as an effective mass $M := m - 2G\sigma$ and $V := G\sigma^2$ in analogy to section 1.2.1, the PNJL-Lagrangian eq. (3.4) is then simplified to:

$$\mathcal{L}_{MFA} = \overline{q} \left(i\gamma_\nu D^\nu - M \right) q - V(\sigma) - \mathcal{U}(\Phi, \overline{\Phi}, T) \tag{3.5}$$

Defining $E(p) := \sqrt{p^2 + M^2}$, $E(p)^\pm := E(p) \pm i\Theta T$ and applying the usual techniques[1], this results in a grand canonical potential at imaginary potential ($i\Theta = i\frac{\mu}{T}$) of the form [8]:

$$\begin{aligned}
&\Omega_{PNJL}(T, \Theta; \Phi, \overline{\Phi}, \sigma) = \\
&\quad V(\sigma) - 2N_f \int \frac{d^3p}{(2\pi)^3} \{ 3E(p) + \\
&\qquad + T \ln \left[1 + 3 \left(\Phi + \overline{\Phi} e^{-\frac{E^-(p)}{T}} \right) e^{-\frac{E^-(p)}{T}} + e^{-\frac{E^-(p)}{T}} \right] + \\
&\qquad + T \ln \left[1 + 3 \left(\overline{\Phi} + \Phi e^{-\frac{E^+(p)}{T}} \right) e^{-\frac{E^+(p)}{T}} + e^{-\frac{E^+(p)}{T}} \right] \} \\
&\quad + \mathcal{U}(\Phi, \overline{\Phi}, \sigma)
\end{aligned} \tag{3.6}$$

This still has a quite similar structure as the thermodynamical potential of the NJL model with the straightforwardly introduced imaginary chemical potential, especially the first term $V(\sigma)$ by definition gives $V = \frac{(M-m)^2}{4G}$ which arises in the NJL potential eq. (2.1) as well. However, in the case of PNJL, instead of the effective mass M, the chiral condensate σ itself shall be introduced as variable, giving an order parameter for the chiral phase transition.

It was found by A. Roberge and N. Weiss in the mid 1980s that in a SU(N) gauge theory at imaginary chemical potential ($\mu = i\Theta T$) the thermodynamic potential Ω as function of Θ shows a periodicity of $\frac{2\pi}{N}$ [8].
In the case at hand, as was mentioned before, this implies a periodicity in Θ with period $\frac{2\pi}{3}$ for the grand canonical potential Ω and the chiral condensate q, which is not reproduced by the straightforward introduction of the imaginary chemical potential in eq. (2.1).
The Polyakov loop Φ itself also does not have this periodicity.

By applying methods of perturbation and lattice theory Roberge and Weiss showed that as functions of Θ the derivative $\frac{d\Omega(\Theta)}{d\Theta}$ and the Polyakov loop Φ become discontinuous for $\Theta = \frac{(2k+1)}{3}\pi$ at high values of T.

[1] Detailed derivations and discussions on the introduction of thermodynamic potentials in QCD can be found in [3]

This behavior outlines the first order Roberge-Weiss (RW) transition which can be associated with the confinement-deconfinement transition.

Following [8] an extended $\mathbb{Z}_3$-transformation that keeps Ω_{PNJL} invariant is introduced:

$$e^{\pm i\Theta} \to e^{\pm i\Theta} e^{\pm i\frac{2\pi k}{3}}, \;\; \Phi(\Theta) \to \Phi(\Theta) e^{-i\frac{2\pi k}{3}}, \;\; \overline{\Phi}(\Theta) \to \overline{\Phi}(\Theta) e^{i\frac{2\pi k}{3}} \tag{3.7}$$

By defining new variables

$$\begin{aligned} \Psi :=& e^{i\Theta}\Phi \\ \overline{\Psi} :=& e^{-i\Theta}\overline{\Phi} \end{aligned} \tag{3.8}$$

this transformation is simplified to (see appendix [B]):

$$e^{\pm i\Theta} \to e^{\pm i\Theta} e^{\pm i\frac{2\pi k}{3}}, \;\; \Psi(\Theta) \to \Psi(\Theta), \;\; \overline{\Psi}(\Theta) \to \overline{\Psi}(\Theta) \tag{3.9}$$

The effective Polyakov loop potential $\mathcal{U}(\Phi, \overline{\Phi}, T)$ is constructed by terms $\overline{\Phi}\Phi$, $\overline{\Phi}^3$ and Φ^3 because of the $\mathbb{Z}_3$ center symmetry $u \xrightarrow{\mathbb{Z}_3} u\, e^{\pm i\frac{2\pi k}{3}}$ [9].
In the present case this is done following [8]:

$$\frac{\mathcal{U}}{T^4} = -\frac{b_2(T)}{2}\overline{\Phi}\Phi - \frac{b_3}{6}\left(\overline{\Phi}^3 + \Phi^3\right) + \frac{b_4}{4}(\overline{\Phi}\Phi)^2 \tag{3.10}$$

with

$$b_2(T) = a_0 + a_1\left(\frac{T_0}{T}\right) + a_2\left(\frac{T_0}{T}\right)^2 + a_3\left(\frac{T_0}{T}\right)^3 \tag{3.11}$$

T_0 denotes the temperature of the deconfinement transition in pure gauge theory which in lattice QCD yields a value of $T_0 = 270\,\mathrm{MeV}$ [8],[9].
The other parameters can then be set by fits to lattice calculations, in [8] the following numbers are used:

a_0	a_1	a_2	a_3	b_3	b_4
6.75	−1.95	2.625	−7.44	0.75	7.5

With the baryonic chemical potential $\mu_B := 3i\Theta T$ the grand canonical potential can now be written as:

$$\begin{aligned} &\Omega_{PNJL}(T, \Theta; \Psi, \overline{\Psi}, \sigma) = \\ &-2N_f \int \frac{d^3p}{(2\pi)^3}\{3E(p) + T\ln\left[1 + 3\Psi e^{-\frac{E(p)}{T}} + 3\overline{\Psi}e^{-2\frac{E(p)}{T}}e^{\frac{\mu_B}{T}} + e^{-3\frac{E(p)}{T}}e^{\frac{\mu_B}{T}}\right] + \\ &\qquad + T\ln\left[1 + 3\overline{\Psi}e^{-\frac{E(p)}{T}} + 3\Psi e^{-2\frac{E(p)}{T}}e^{-\frac{\mu_B}{T}} + e^{-3\frac{E(p)}{T}}e^{-\frac{\mu_B}{T}}\right]\} \\ &\quad + V(\sigma) + \left[-\frac{b_2(T)}{2}T^4\overline{\Psi}\Psi - \frac{b_3}{6}T^4\left(\overline{\Psi}^3 e^{\frac{\mu_B}{T}} + \Psi^3 e^{-\frac{\mu_B}{T}}\right) + \frac{b_4}{4}T^4(\overline{\Psi}\Psi)^2\right] \end{aligned} \tag{3.12}$$

which is obviously invariant under transformation (3.9) as
$e^{\pm i\frac{\mu_B}{T}} = e^{\pm 3i\Theta} \xrightarrow{ext.\ \mathbb{Z}_3} e^{\pm 3i\Theta} e^{\pm i2\pi k} = e^{\pm 3i\Theta}$.
For $\Theta \to \Theta + \frac{2\pi}{3}$ the potential eq. (3.12) keeps the same form if $\Psi(\Theta)$ and $\overline{\Psi}(\Theta)$ are replaced by $\Psi(\Theta + \frac{2\pi}{3})$ and $\overline{\Psi}(\Theta + \frac{2\pi}{3})$, following [8] this implies:

$$\Psi(\Theta) = \Psi(\Theta + \frac{2\pi}{3}), \quad \overline{\Psi}(\Theta + \frac{2\pi}{3}) = \overline{\Psi}(\Theta) \tag{3.13}$$

This eventually shows the expected RW-periodicity of $\frac{2\pi}{3}$, such that as function of Θ the PNJL potential complies with $\Omega_{PNJL}(\Theta + \frac{2\pi}{3}) = \Omega_{PNJL}(\Theta)$.

3.3 Gap equations

To find the minimum of this grand canonical potential $\Omega_{PNJL}(T, \Theta; \Psi, \overline{\Psi}, \sigma)$ for fixed values (T, Θ) it is necessary to evaluate the derivatives $\frac{\partial\Omega_{PNJL}}{\partial\sigma}$, $\frac{\partial\Omega_{PNJL}}{\partial\psi}$ and $\frac{\partial\Omega_{PNJL}}{\partial\overline{\psi}}$, which effectively are the gradient components of Ω_{PNJL} in domains of (σ, ψ, $\overline{\psi}$).
For $\psi = e^{i\Theta}\Phi$ and $\overline{\psi} = e^{-i\Theta}\overline{\Phi}$ it is convenient to assign the Polyakov loop Φ, $\overline{\Phi}$ modulus $A := |\Phi| = |\overline{\Phi}| = |\Psi|$ and phase ν: $\Phi = Ae^{i\nu}$, $\overline{\Phi} = Ae^{-i\nu}$, such that

$$\begin{aligned} \Psi &= Ae^{i(\nu+\Theta)} \\ \overline{\Psi} &= Ae^{-i(\nu+\Theta)} \end{aligned} \tag{3.14}$$

in accordance to (3.8).

So Ω_{PNJL} is given by a function of $(T, \Theta; A, \nu, \sigma)$[1]:

$$\begin{aligned} &\Omega_{PNJL}(T, \Theta; A, \nu, \sigma) = \\ &-2N_f \int \frac{d^3p}{(2\pi)^3} \{3E(p) + \\ &\quad + T\ln\left[1 + 3Ae^{i(\nu+\Theta)}e^{-\frac{E(p)}{T}} + 3Ae^{-(\nu+\Theta)}e^{-2\frac{E(p)}{T}}e^{\frac{\mu_B}{T}} + e^{-3\frac{E(p)}{T}}e^{\frac{\mu_B}{T}}\right] + \\ &\quad + T\ln\left[1 + 3Ae^{-i(\nu+\Theta)}e^{-\frac{E(p)}{T}} + 3Ae^{(\nu+\Theta)}e^{-2\frac{E(p)}{T}}e^{-\frac{\mu_B}{T}} + e^{-3\frac{E(p)}{T}}e^{-\frac{\mu_B}{T}}\right]\} \\ &+ G\sigma^2 + \left[-\frac{b_2(T)}{2}T^4A^2 - \frac{b_3}{3}T^4A^3\cos(3\nu) + \frac{b_4}{4}T^4A^4\right] \end{aligned} \tag{3.15}$$

where $E(p) = \sqrt{p^2 + M^2} = \sqrt{p^2 + (m - 2G\sigma)^2}$, therefore also dependent of σ.

So the gap equations for this thermodynamic potential are eventually obtained in analogy to eq. (1.18) by the derivatives $\frac{\partial\Omega_{PNJL}}{\partial A}$, $\frac{\partial\Omega_{PNJL}}{\partial\nu}$ and $\frac{\partial\Omega_{PNJL}}{\partial\sigma}$.
As those are quite extensive, they are given in appendix [D].

[1] for the arise of the cos-term in the Polyakov potential see appendix [C]

The further approach is the same as for the NJL model in the previous chapter. However, it is now necessary to solve a system of three gap equations for fixed values (T, Θ) to obtain the physical values of A, ν and σ minimizing the grand canonical potential Ω_{PNJL}.
As the numerical calculations take much more time than for the simple NJL model and did not yield reasonable results, the further investigation of the PNJL model was not possible by the time of this thesis.
Nonetheless, by finding the physical values (A, ν, σ) it would eventually be possible to compile more elaborated phase diagrams including the chiral phase transition as well as the confinement-deconfinement transition. Some ideas of the transition behavior as well as diagrams in domains of T and Θ (or μ) are given in [8] and [14].

Chapter 4

Conclusion

The obtained results in sections 2.1 and 2.2 match expectations for the NJL model well, unfortionately effective calculations for the extended PNJL approach were not feasible in this work due to time constraints and problems with the numerical computation of the system of gap equations in 3.3.
The NJL results, especially at imaginary chemical potential, might probably be improved by investigating the intervals in domains of T and μ or Θ more precisely by simply computing more points of the phase transition (T, μ) or (T, Θ) respectively. This should give a smoother behavior in the unphysical regime of the p-T-diagrams.
Looking at the right hand side of fig. 2.1 it should actually be possible to narrow down the found crossover transition up to zero chemical potential by investigating the slope behavior in direction of the T-axis. The slope was here examined in μ direction and the transition was neglected below reasonably high values. Extending this crossover transition would also give more insight on the behavior of the transition from the physical to unphysical domain in the upper p-T-diagram of fig. 2.9.
The fact that for the chiral limit $m = 0$ the transition points in fig. 2.9 behave smoothly at the limiting line between the realms of real and imaginary chemical potential is an interesting insight that was not predicted before the actual calculations. This also shows an advantage of the portrayal of the QCD phases in domains of (p, T), especially when dealing with real and imaginary μ, as fig. 2.4 and 2.8 in domains of $T, \mu)$ and (T, Θ) do not show this connectedness between the results of physical and unphysical μ straightaway.

Chapter 5

Appendix

[A] As the complex exponential functions only appear in the ln-terms, those shall be analyzed:

$$\begin{aligned}
&\ln\left[1+e^{-\frac{E(p)}{T}}e^{-i\Theta}\right]+\ln\left[1+e^{-\frac{E(p)}{T}}e^{i\Theta}\right]= \\
&=\ln\left[(1+e^{-\frac{E(p)}{T}}e^{-i\Theta})(1+e^{-\frac{E(p)}{T}}e^{i\Theta})\right]= \\
&=\ln\left[1+e^{-\frac{E(p)}{T}}(e^{i\Theta}+e^{-i\Theta})+e^{-2\frac{E(p)}{T}}\right]= \\
&=\ln\left[1+2\cos\Theta\ e^{-\frac{E(p)}{T}}+e^{-2\frac{E(p)}{T}}\right]
\end{aligned}$$

This gives strictly real values, therefore the potential Ω_{NJL} is a real function. It also explains the mirrored behavior discussed for fig. 2.5 and 2.7, as the cos-term reflects the found symmetry $M(T,\Theta)=M(T,2\pi-\Theta)$.

[B] The extended $\mathbb{Z}_3$ transformation is given as:

$$e^{\pm i\Theta}\to e^{\pm i\Theta}e^{\pm i\frac{2\pi k}{3}} \tag{5.1}$$

$$\Phi(\Theta)\to\Phi(\Theta)e^{-i\frac{2\pi k}{3}} \tag{5.2}$$

$$\overline{\Phi}(\Theta)\to\overline{\Phi}(\Theta)e^{i\frac{2\pi k}{3}} \tag{5.3}$$

so Ψ and $\overline{\Psi}$ are transformed:

$$\Psi(\Theta)=e^{i\Theta}\Phi(\Theta)\xrightarrow{(5.1),(5.2)}\left(e^{i\Theta}e^{i\frac{2\pi k}{3}}\right)\left(\Phi(\Theta)e^{-i\frac{2\pi k}{3}}\right)=e^{i\Theta}\Phi(\Theta)=\Psi(\Theta)$$

$$\overline{\Psi}(\Theta)=e^{-i\Theta}\overline{\Phi}(\Theta)\xrightarrow{(5.1),(5.3)}\left(e^{-i\Theta}e^{-i\frac{2\pi k}{3}}\right)\left(\overline{\Phi}(\Theta)e^{i\frac{2\pi k}{3}}\right)=e^{-i\Theta}\overline{\Phi}(\Theta)=\overline{\Psi}(\Theta)$$

[C] Introducing $\Psi := Ae^{i(\nu+\Theta)}$, $\overline{\Psi} := Ae^{-i(\nu+\Theta)}$ in (3.12) gives:

$$
\begin{aligned}
&\Omega_{PNJL}(T,\Theta;A,\nu,\sigma) = \\
&-2N_f \int \frac{d^3p}{(2\pi)^3}\{3E(p)+ \\
&\quad + T\ln\left[1+3Ae^{i(\nu+\Theta)}e^{-\frac{E(p)}{T}}+3Ae^{-(\nu+\Theta)}e^{-2\frac{E(p)}{T}}e^{\frac{\mu_B}{T}}+e^{-3\frac{E(p)}{T}}e^{\frac{\mu_B}{T}}\right]+ \\
&\quad + T\ln\left[1+3Ae^{-i(\nu+\Theta)}e^{-\frac{E(p)}{T}}+3Ae^{(\nu+\Theta)}e^{-2\frac{E(p)}{T}}e^{-\frac{\mu_B}{T}}+e^{-3\frac{E(p)}{T}}e^{-\frac{\mu_B}{T}}\right]\} \\
&+G\sigma^2 \\
&+\left[-\frac{b_2(T)}{2}T^4A^2-\underline{\frac{b_3}{6}T^4A^3\left(e^{-3i(\nu+\Theta)e^{\frac{\mu_B}{T}}}+e^{3i(\nu+\Theta)}e^{-\frac{\mu_B}{T}}\right)}+\frac{b_4}{4}T^4A^4\right]
\end{aligned}
$$

where the underlined term of the effective Polyakov potential can be simplified to (note that $\frac{\mu_B}{T} = 3i\Theta$):

$$
\begin{aligned}
&\frac{b_3}{6}T^4A^3\left(e^{-3i(\nu+\Theta)e^{\frac{\mu_B}{T}}}+e^{3i(\nu+\Theta)}e^{-\frac{\mu_B}{T}}\right) \\
&\quad = \frac{b_3}{6}A^3\left(e^{-3i\nu}+e^{3i\nu}\right) \\
&\quad = \frac{b_3}{3}T^4\cos(3\nu)
\end{aligned}
$$

[D] Gap equations for the PNJL model eq. (3.15)

$$
\begin{aligned}
&\frac{\partial\Omega_{PNJL}}{\partial A} = \\
&-2N_f\int\frac{d^3p}{(2\pi)^3}\,3T\{\frac{e^{i(\nu+\Theta)}e^{-\frac{E(p)}{T}}+e^{-i(\nu+\Theta)}e^{-2\frac{E(p)}{T}}e^{\frac{\mu_B}{T}}}{1+3Ae^{i(\nu+\Theta)}e^{-\frac{E(p)}{T}}+3Ae^{-(\nu+\Theta)}e^{-2\frac{E(p)}{T}}e^{\frac{\mu_B}{T}}+e^{-3\frac{E(p)}{T}}e^{\frac{\mu_B}{T}}}+ \\
&\qquad\qquad + \frac{e^{-i(\nu+\Theta)}e^{-\frac{E(p)}{T}}+e^{i(\nu+\Theta)}e^{-2\frac{E(p)}{T}}e^{-\frac{\mu_B}{T}}}{1+3Ae^{-i(\nu+\Theta)}e^{-\frac{E(p)}{T}}+3Ae^{(\nu+\Theta)}e^{-2\frac{E(p)}{T}}e^{-\frac{\mu_B}{T}}+e^{-3\frac{E(p)}{T}}e^{-\frac{\mu_B}{T}}}\} \\
&+\left[-b_2(T)T^4A-b_3T^4A^2\cos(3\nu)+b_4T^4A^3\right]
\end{aligned}
$$

$$\frac{\partial \Omega_{PNJL}}{\partial \nu} =$$

$$-2N_f \int \frac{d^3p}{(2\pi)^3}\, 3TiA\{\frac{e^{i(\nu+\Theta)}e^{-\frac{E(p)}{T}} - e^{-i(\nu+\Theta)}e^{-2\frac{E(p)}{T}}e^{\frac{\mu_B}{T}}}{1+3Ae^{i(\nu+\Theta)}e^{-\frac{E(p)}{T}} + 3Ae^{-(\nu+\Theta)}e^{-2\frac{E(p)}{T}}e^{\frac{\mu_B}{T}} + e^{-3\frac{E(p)}{T}}e^{\frac{\mu_B}{T}}} +$$

$$+ \frac{e^{i(\nu+\Theta)}e^{-2\frac{E(p)}{T}}e^{-\frac{\mu_B}{T}} - e^{-i(\nu+\Theta)}e^{-\frac{E(p)}{T}}}{1+3Ae^{-i(\nu+\Theta)}e^{-\frac{E(p)}{T}} + 3Ae^{(\nu+\Theta)}e^{-2\frac{E(p)}{T}}e^{-\frac{\mu_B}{T}} + e^{-3\frac{E(p)}{T}}e^{-\frac{\mu_B}{T}}}\}$$

$$+ b_3 T^4 A^3 \sin(3\nu)$$

$$\frac{\partial \Omega_{PNJL}}{\partial \sigma} =$$

$$-2N_f \int \frac{d^3p}{(2\pi)^3}\, 3\{-\frac{4G(m-2G\sigma)}{E(p)} +$$

$$+ \frac{\frac{4G(m-2G\sigma)}{E(p)}Ae^{i(\nu+\Theta)}e^{-\frac{E(p)}{T}} + 2\frac{4G(m-2G\sigma)}{E(p)}Ae^{-i(\nu+\Theta)}e^{-2\frac{E(p)}{T}}e^{\frac{\mu_B}{T}} + \frac{4G(m-2G\sigma)}{E(p)}e^{-3\frac{E(p)}{T}}e^{\frac{\mu_B}{T}}}{1+3Ae^{i(\nu+\Theta)}e^{-\frac{E(p)}{T}} + 3Ae^{-(\nu+\Theta)}e^{-2\frac{E(p)}{T}}e^{\frac{\mu_B}{T}} + e^{-3\frac{E(p)}{T}}e^{\frac{\mu_B}{T}}} +$$

$$+ \frac{\frac{4G(m-2G\sigma)}{E(p)}Ae^{-i(\nu+\Theta)}e^{-\frac{E(p)}{T}} + 2\frac{4G(m-2G\sigma)}{E(p)}Ae^{i(\nu+\Theta)}e^{-2\frac{E(p)}{T}}e^{-\frac{\mu_B}{T}} + \frac{4G(m-2G\sigma)}{E(p)}e^{-3\frac{E(p)}{T}}e^{-\frac{\mu_B}{T}}}{1+3Ae^{-i(\nu+\Theta)}e^{-\frac{E(p)}{T}} + 3Ae^{(\nu+\Theta)}e^{-2\frac{E(p)}{T}}e^{-\frac{\mu_B}{T}} + e^{-3\frac{E(p)}{T}}e^{-\frac{\mu_B}{T}}}\}$$

$$+ 2G\sigma$$

Bibliography

[1] M. Buballa. *NJL-model analysis of dense quark matter.* Physics Reports 407:205, 2005.

[2] P. Schmüser. *Feynman-Graphen und Eichtheorien fr̈ Experimentalphysiker.* Springer, 1995.

[3] J. I. Kapusta. *Finite Temperature Field Theory.* Cambridge University Press, 1989.

[4] J. Wambach, K. Heckmann, M.Buballa. *Transport Properties of Strong-Interaction Matter.* 5:909, 2012.

[5] H. Fritzsch, M. Gell-Mann, H. Leutwyler. Phys. Lett. 47B:365, 1973

[6] Y. Nambu and G. Jona-Lasinio. *Dynamical model of elementary particles based on an analogy with superconductivity. I.* Physical Review 122:345, 1961.

[7] Y. Nambu and G. Jona-Lasinio. *Dynamical model of elementary particles based on an analogy with superconductivity. II.* Physical Review 124:246, 1961.

[8] Y. Sakai, K. Kashiwa, H. Kouno, M. Yahiro. *Polyakov loop extended NJL model with imaginary chemical potential.* 2007. http://arxiv.org/abs/0801.0034v1

[9] W. Weise, C. Ratti, S. Rössner. *Phases of QCD, Polyakov Loop and Quasiparticles.* 2007. http://arxiv.org/abs/0704.3585v1

[10] P. Finelli. *Nuclear Physics Course: Chiral Symmetry.* Physics Department, University of Bologna, 2011.

[11] P. de Forcrand. *Simulating QCD at finite density.* PoS(LAT2009)010, 2009. http://xxx.lanl.gov/abs/1005.0539

[12] J. Bloch, T. Wettig. *The QCD sign problem and dynamical simulations of random matrices.* 2011. http://arxiv.org/abs/1102.3715

[13] L. Fister, J. M. Pawlowski. *Quark Confinement from Correlation Functions.* 2012.
http://arxiv.org/abs/1302.1373

[14] D. Scheffler. *The PNJL model at imaginary chemical potential.* Darmstadt, 2010